WEAK TEMPERATURE DEPENDENCE OF STRUCTURE IN HYDROPHOBIC POLYELECTROLYTE AQUEOUS SOLUTION (PSSNa) : CORRELATION BETWEEN SCATTERING AND VISCOSITY ‡

Wafa ESSAFI[1,*], Nouha HABOUBI[1,2], Claudine WILLIAMS[3] and Francois BOUÉ[4]

1 Institut National de Recherche et d'Analyse Physico-Chimique, Pôle Technologique de Sidi Thabet, 2020 Sidi Thabet - Tunisie

2 Faculté des Sciences de Tunis-Département de Chimie, Campus Universitaire, 2092 El Manar Tunis-Tunisie

3 Physique de la Matière Condensée, UMR 7125 CNRS - Collège de France, 11 Place Marcelin Berthelot, F 75321 Paris, France

4 Laboratoire Léon Brillouin, UMR 12 CNRS - IRAMIS CEA Saclay, 91191 Gif sur Yvette Cedex, France

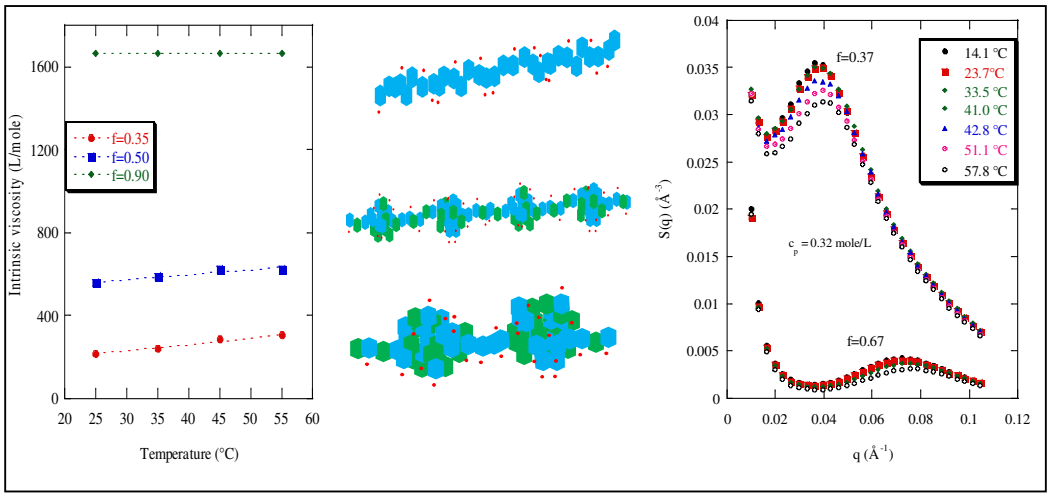

PACS Numbers :
82.35.Rs : Polyelectrolytes

82.35.-x : Polymers: properties; reactions; polymerization

83.85.Hf : X-ray and neutron scattering

66.20.-d : Viscosity

Abstract

We study in this paper, either in the semi-dilute regime by small angle scattering or in dilute and semi-dilute unentangled regime by viscosimetric measurements, the influence of temperature on the structure of aqueous solutions of a hydrophobic polyelectrolyte,

poly(styrene-co-sodium styrene sulfonate). There is a strong consistency between the two methods: the very weak dependence over temperature at high chemical charge is increased for lower charge fractions i.e. when hydrophobicity is increased. The solvent quality is thus modified, whereas, for comparison, the hydrophilic polyelectrolyte poly(acrylamide-co-sodium-2-acrylamido-2-methylpropane sulfonate), shows a structure totally independent on temperature, for all the charge fractions.

Poly(styrene-co-sodium styrene sulfonate) (PSSNa)
Poly(acrylamide-co-sodium-2-acrylamido-2-methylpropane sulfonate) (AMAMPS)

‡ This paper is dedicated to the very fond memory of Claudine Williams, who is behind the investigation of this new class of polyelectrolytes.

* Corresponding author. Tel.: +216 21 19 55 23; fax: +216 71 53 76 88; e-mail address: wafa.essafi@wanadoo.fr

I-INTRODUCTION :

Polyelectrolytes are polymers containing ionisable groups. Once dissolved in suitable polar solvent such as water, the ion pairs dissociate into charges linked to the polymer backbone and counter-ions dispersed in whole the solution. Polyelectrolytes are called hydrophobic when water is a poor solvent for the backbone ($T < \Theta$ temperature); the process of their solvation is then a combination of electrostatic and hydrophobic interactions. Conversely, backbones of hydrophilic polyelectrolytes are under good solvent conditions in water ($T >> \Theta$ temperature) and interactions have mainly a pure electrostatic nature.

In the dilute regime and for good ($T >> \Theta$) and Θ solvents, the single chain is described as an extended (rodlike) configuration of electrostatic blobs. [1] For the hydrophobic polyelectrolytes ($T < \Theta$ temperature), the single chain properties are described in the framework of the pearl-necklace model, [2-4] as forming compact beads (the pearls) joined by narrow elongated strings. Experimentally, the presence of hydrophobic domains (beads) in dilute hydrophobic polyelectrolyte solutions such as PSS in aqueous solutions was already highlighted in previous papers. [5] Inside the beads, the local dielectric constant ε can be very low, what causes a reduction of osmotically active counterions. [6]

In the semi-dilute regime where many chains interact with each others, in good and Θ solvents the polyelectrolyte chain is a random walk of correlation blobs, [7,1] each blob is an extended configuration of electrostatic blobs, and the correlation length ξ i.e. the mesh size of the isotropic transient network of overlapping chains scales as $c_p^{-1/2}$ where c_p is the polyelectrolyte concentration. Experimentally, the evolution of ξ with c_p was verified for highly charged hydrophilic polyelectrolyte. [8,9,10] In the case of hydrophobic polyelectrolyte two regimes have been predicted by Dobrynin et al [4]: the string controlled regime and the bead-controlled regime. The string controlled regime exists as long as the pearl size is much

smaller than the correlation length ξ; a classical polyelectrolyte behaviour is expected where ξ scales as $c_p^{-1/2}$. When the pearl size becomes of the order of ξ, a bead-controlled semi-dilute regime is expected with ξ scales as $c_p^{-1/3}$ and the system behaves as a solution of charged beads of constant size. Experimentally, two regimes with two scaling exponents being –1/2 and –1/7 have been observed for a solvophobic polyelectrolyte in nonaqueous solvent. [11] For the model hydrophobic PSS in water, the total structure function was measured by Small Angle Scattering studies (SAXS and SANS) and it was found that ξ scales as $c_p^{-\alpha}$ where α decreases from 0.5 to less than 0.4 when decreasing the chemical charge fraction of the chain *f*. [12,13] Later, this was also observed by Baigl et al. through SAXS and Atomic Force Microscopy studies. [14,15] Finally, the counterion condensation in aqueous hydrophobic polyelectrolyte solutions has been studied experimentally through ξ and it was found that the effective charge is strongly reduced [6], compared to the hydrophilic case [16,17] as explained recently since the pearls can be penetrable to the counterions.[18] Concerning the effect of the solvent quality – i.e. of the level of attractive contribution, it can be decreased compared to water by using solvent mixtures of variable composition, like adding acetone to water for a hydrophilic polyelectrolyte[19,20]; it has been concluded in this case that the polyelectrolyte chain undergoes a coil to globule collapse transition [19,20]. Conversely, for a hydrophobic polyelectrolyte, the effect of increasing solvent quality was investigated experimentally either by using one mixture of water and an organic solvent, THF [21], which is also slightly polar, or by using a polar organic solvent of good quality for the backbone allowing at the same time significant ionic dissociation. [22,21] In the first case when THF is added, [21] the chain conformation evolves from the pearl necklace shape already reported in pure water, towards the conformation in pure water for fully sulfonated PSS, which is string-like as also reported previously. The second case results in a classical polyelectrolyte-like behaviour, as shown for polyelectrolyte in semi-dilute non aqueous solvent [11,21] and it was found that the correlation length ξ scales as $c_p^{-1/2}$ as expected for good solvents. [4,23]

Another way to control the solvent quality and so the balance between electrostatic and hydrophobic interactions is to modify the temperature. Experimentally, the variation of temperature on aqueous polyelectrolyte solutions has been applied by Boué et al [24] on fully sulfonated PSSNa semi-dilute solutions, showing no effect of temperature on both inter and intrachain interactions. [24] The aim of the present work is to investigate the effect of temperature on the structure of aqueous solutions of sulfonated PSSNa at intermediate charge fractions, thus increasing the hydrophobicity of the highly charged polyelectrolyte:

- either by Small Angle Scattering (SAXS and SANS) in the semi dilute regime and thus we determine the total structure function,
- or by viscosimetric measurements in the dilute and semi-dilute unentangled regimes, allowing the determination of the intrinsic viscosity of the different polyelectrolytes as a function of temperature.

For comparison, we will study also the behaviour of AMAMPS, a polyelectrolyte in good solvent in water, at the same intermediate charge fractions.

II-MATERIAL & METHODS:

II-1-Polymer synthesis and characterization

The hydrophobic polyelectrolyte used in this study is a copolymer of styrene and sodium styrene sulfonate [poly-(sodium styrene sulfonate)$_f$ - (styrene)$_{1-f}$)] (PSSNa) whose chemical structure is shown on figure 1. It was prepared by post-sulfonation of polystyrene based on the Makowski procedure [25, 12], which enables partial sulfonation and leads to a well-defined polyelectrolyte. [26]

The Makowski procedure [25] is a phase transfer, interfacial, reaction. A commercial polystyrene (M_w = 250,000 g/mole and a polydispersity = 2 for SAXS and SANS mesurements, M_w = 280,000 g/mole of batch n° 16311DB of Sigma-Aldrich Reference 182427, for viscometric measurements) was disssolved in dichloroethane and mixed at a temperature of 50 °C with acetic acid and sulfuric acid in proportions depending on the desired fraction of charge. A white layer appears between the two media. After 30 to 60 min, the aqueous phase is neutralized with sodium hydroxide, dialyzed against deionized water until the conductivity of the external dialysis bath remains stable. The solutions are then concentrated with a rotating evaporator and finally freeze-dried. The resulting white powder is better stored away from light and was characterized by elemental microanalysis of carbon, sulfur and sodium to determine the degree of sulfonation *f* of the polyelectrolytes. It was varied between 0.3 (the limit for solubility in water) and 1 (fully charged). The degree of sulfonation *f* is thus always above the Manning condensation limit for the charge fraction, equal to $a/l_B \sim 0.3$ for PSS in water (a, length of one unit, $l_B \sim 7$ Å, Bjerrüm length in water).

The hydrophilic polyelectrolyte also studied in this paper is [poly(sodium-2-acrylamido-2-methylpropane sulfonate)$_f$ -(acrylamide)$_{(1-f)}$], whose chemical structure is shown on figure 1. The average molar mass of the monomer is 71 +158**f*. It was synthesized by radical copolymerisation of acrylamide with 2-acrylamido-2-methyl propane sulfonic acid, a method reported formerly [27] which was slightly modified by adjusting the ratio of the two

monomers to obtain, after neutralisation, a fraction of ionisable units (AMPS), *f*, between 0.30 and 1. Thus these chains are also highly charged polyelectrolytes. The resulting molecular weight is M_w = 650,000 g/mole (N_w = 2800) and the polydispersity is 2.6, for f = 0.95. Note that both polyelectrolytes (AMAMPS and PSS) are salts of strong acid, bearing SO_3^- anions as side groups when ionised, with Na^+ counterions. So the two polyelectrolytes used in this study differ mainly by the solvation characteristics of their backbone (hydrophobic in the case of PSS, hydrophilic in the case of AMAMPS).

II-2. Preparation of solutions

Solutions were prepared by dissolving dry polyelectrolyte in the solvent and letting at rest for two days before measurements. For SAXS measurements, the solvent is deionised H_2O and for the SANS measurements, the solvent is D_2O used as delivered (Eurisotop).

All concentrations are expressed in moles per liter of the corresponding monomer.

II-3-SAXS measurements

Small Angle X-ray Scattering (SAXS) experiments were performed on beam line D22, at LURE, using the DCI synchrotron radiation source. Data were obtained with pinhole collimation and recorded with a linear detector of 512 cells. The scattering vector q varied from 0.008 to 0.2 $Å^{-1}$ [$q = (4\pi/\lambda)\ sin(\theta/2)$, where θ is the observation angle and λ, the wavelength was 1.37 Å]. The scattering data were normalized to constant beam intensity and corrected for transmission, sample thickness, parasitic and background scattering. The resulting scattering profiles are obtained as normalized intensities in relative units versus scattering vector q.

II-4-SANS measurements

Small Angle Neutron Scattering (SANS) measurements were performed on the PACE spectrometer at the Orphée reactor of LLB, CEA- Saclay, France (www-llb.cea.fr). The q-range was varied between 0.0098 and 0.1046 $Å^{-1}$, the used set-up was characterised by the distance sample to detector D = 2 m and a wavelength λ = 9.52 Å set by a velocity selector. The scattered intensity was recorded by a multidetector with 30 concentric, 1 cm wide rings. The response of each ring was normalized to the (flat) incoherent scattering of light water. Samples were contained in 2 mm thick quartz cells.

The recorded intensity was corrected for sample thickness, transmission, incoherent and background scattering (the solvent contribution). Using direct beam measurements of Cotton method, [28] the intensities were obtained in absolute units of cross-section; they were then divided by the contrast factor. The SANS data are plotted as $S(q)$ versus q.

II-5-VISCOSITY measurements

Viscometric measurements of the polyelectrolyte solutions were carried out with an Ubbelohde tube of 0.84 mm diameter by using a SCHOTT viscometer (AVS 470).

All polyelectrolyte solutions were made up in deionised H_2O, prepared two days before using and filtered just before measurement with an hydrophilic syringe filter of 5 μm porosity. Each solution was kept about 15 minutes in the bath prior to the measurements, for temperature equilibrium.

III-RESULTS:

III-1-Small Angle Scattering study in semi-dilute regime

III-1-a- Effect of temperature on a hydrophilic polyelectrolyte

Figure 2 shows the evolution of the SAXS profiles with temperature in a range between 25 and 55°C, for the AMAMPS aqueous solutions in the semi-dilute regime, at different charge fractions. The polyelectrolyte concentration is kept equal to 0.32 mole/L, for all the samples.

It emerges that the scattering function is independent of the temperature for all the charge fractions, in shape and in intensity. Namely, the position of the peak is unchanged as well as its intensity and the scattered intensity at zero angle is constant with the temperature.

So, for the hydrophilic polyelectrolyte AMAMPS aqueous solutions in the semi-dilute regime, the structure function is independent of temperature for all the charge fractions indicating that the solvent quality is not improved as the temperature increases. This is perfectly in agreement with a simple polyelectrolyte model where only electrostatics play a role (see Discussion).

III-1-b- Effect of temperature on a hydrophobic polyelectrolyte

The effect of temperature on the structure properties of the hydrophobic polyelectrolyte PSS aqueous solutions has been investigated either by SAXS (Figure 3a) or by SANS (Figure 3b), for different charge fractions $f < 1$ in the semi-dilute regime. It emerges that the evolution for SAXS and SANS profiles is slightly different though essentially similar.

For lower charge fractions - $f = 0.35$ in Figure 3a, and 0.37 (Figure 3b), a clear cut result is that the scattered intensity of the peak **decreases as the temperature increases**. This is common to SAXS and SANS profiles. The results are slightly different for the position of the peak: it varies (increases slightly) in the SANS data, while this is not detectable in the SAXS data; this may be because the resolution of the X-ray measurements is lower here, at variance with the most common situation, so that we will trust the SANS.

For f = 0.65 (Figure 3b), the behaviour is similar than for f = 0.35, but less pronounced; the height and position of the peak still depend on temperature as for lower f.

For f = 0.82, the changes are much weaker; they however follow the same trend.

Both intensity decrease and q* increase are consistent: they could be associated to a lower distance between polyelectrolyte strands of lower linear mass (or necklaces with smaller pearls).

In summary our experimental results for hydrophobic PSSNa show a visible effect on the scattering intensity of the maximum, and a weak dependence of q* with the temperature, detectable only by SANS. The structure of the semi-dilute polyelectrolyte solutions depends very weakly on temperature showing that the solvent quality is slightly improved with increasing the temperature.

III-2- Viscometric study in dilute and semi-dilute unentangled regimes

III-2-a- Hydrophilic polyelectrolyte

The variation of the reduced viscosity versus the concentration of AMAMPS $f = 0.95$ in water for different temperatures, is presented in figure 4. For all temperatures, the curves show a polyelectrolyte behaviour in water that is a typical upturn of the reduced viscosity $\eta_{red} = f(c_p)$ at low concentrations. As the polymer concentration decreases, the Debye length increases resulting in an increase of intramolecular repulsive interactions. Thus the expansion of the polyelectrolyte chain takes place and, consequently, η_{red} increases.

It emerges that the reduced viscosity is independent of the temperature for the AMAMPS $f = 0.95$ in water.

III-2-b- Hydrophobic polyelectrolyte:

Figure 5 shows the evolution of the reduced viscosity versus the concentration for PSSNa in water at 25°C, for different charge fractions.

For all charge fractions, the PSSNa presents a typical behaviour of polyelectrolyte: the reduced viscosity increases as the concentration decreases, as seen earlier for the hydrophilic polyelectrolyte in water. Under the effect of dilution, the screening of electrostatic charges by the counter-ions along the chain is reduced and the intramolecular repulsive interactions between charges along the chain are increased, which leads to an expansion of the polyelectrolyte chain, and so inducing an increase in reduced viscosity. [30,31]

The effect of temperature increase for the different PSSNa aqueous solutions is shown on Figure 6. Figure 6a shows that for the highly charged PSS (f = 0.90), the reduced viscosity is independent of the temperature and the polyelectrolyte behaves as a hydrophilic one. On the contrary, when f decreases (for f = 0.50 and even more for f = 0.35, Fig. 6b and 6c), the

reduced viscosity increases slightly with temperature. This result shows an increase of the hydrodynamic volume of the PSSNa with temperature, attributed to a slight improve of the solvent quality. This behaviour is more pronounced as the charge fraction decreases, indicating that the solvent quality is improved as the charge fraction increases.

Thus viscosimetric results are sensitive, as well as scattering results to the temperature changes applied here.

IV DISCUSSION:

IV-1-Small Angle Scattering study in semi-dilute regime

IV-1-a- Effect of temperature on a hydrophilic polyelectrolyte

Concerning the hydrophilic polyelectrolyte, it emerges firstly that for all the charge fractions the peak position, q*, does not depend on the temperature, which shows that the polyelectrolyte chain network of the AMAMPS has its mesh size unchanged. Secondly the constancy of the peak intensity suggests that the effective charge remains constant with temperature (for the SAXS data discussed here, the contrast comes from sulfur and also from the condensed sodium counter-ions (which bring electrons for a small additional volume). Thirdly the constancy of the width of the peak confirms that the order degree of the system remains also constant with the temperature. And finally the fact that the scattered intensity at zero angle is constant with the temperature, also supports the idea that the effective charge is constant: the scattered intensity at zero angle is related to the osmotic compressibility as, according the Dobrynin model[2] :

$$S(q \to 0) \approx kTc_p \frac{\partial c_p}{\partial \Pi} \approx c_p / f_{eff} \qquad \text{(Eq.1)}$$

The absence of low q upturn signals the absence of large hydrophobic aggregates, which would have been likely to evolve with temperature. So, the chain network structure is independent of temperature for the hydrophilic polyelectrolyte.

In the context of Manning-Oosawa theory, [16,17] the effective charge is expressed as :

$$f_{eff} = \frac{a}{|z| l_B} \qquad \text{(Eq.2)}$$

where a is the monomer size which is considered as independent on T, z the charge of the ion (equal to 1 in our case) and l_B is the Bjerrum length :

$$l_b = \frac{e^2}{4\pi\varepsilon\varepsilon_0 k_B T} \quad \text{(Eq. 3)}$$

with T : the temperature in Kelvin.

k_B : Boltzmann constant = 1,38. 10^{-23} J.°K^{-1}.

ε: the relative dielectric constant of the medium (solvent).

ε_0: is the vacuum permittivity

e: elementary electrostatic charge = 1,6. 10^{-19} C.

In water at 25 °C, ε = 78 and so l_b = 7 Å.

This gives:

$$f_{eff} \propto l_B^{-1} \propto \varepsilon T \qquad \text{(Eq.4)}$$

To take into account the evolution of the solvent dielectric constant ε with temperature in the range between 0 and 100°C, we use data for ε available in reference [29] and put them in the form of an effective scaling law: we find

$$\varepsilon \propto T^{-1.47} \qquad \text{(Eq.5)}$$

and therefore the effective charge scales as :

$$f_{eff} \propto l_B^{-1} \propto T^{-0.47} \qquad \text{(Eq.6)}$$

Note that such a variation is weak since the explored range of temperature is limited between 25°C (298 °K) and 55°C (328 °K). This explains the apparent constancy of the effective charge with temperature and by consequence the invariance of the scattered intensity at zero angle $S(q \to 0)$ with temperature.

The dependence of q* is predicted by the theoretical models describing the structure of the semi-dilute classical polyelectrolyte solutions derived from the isotropic phase model, first introduced by de Gennes and co [7] and later by Dobrynin and co [1] which is characterized for polyelectrolytes in good solvents, by a correlation length ξ. Thus the position q* of the maximum in the scattering intensity profile scales as :

$$q^* \propto \left(\frac{B}{c_p a}\right)^{-1/2} \propto \left(\frac{l_B}{a}\right)^{1/7} f_{eff}^{2/7} (c_p a)^{1/2} \qquad \text{for } T >> \Theta \qquad \text{(Eq.7)}$$

where *B* is a parameter including the solvent quality. The dependence in T is contained in the dependence over l_B

$$q^* \propto l_B^{-1/7} \propto T^{-0.067} (c_p a)^{1/2} \qquad \text{for } T >> \Theta \qquad \text{(Eq.8)}$$

taking into account the evolution of ε with T of (Eq.5).[29] q* should decrease with temperature, but its relative variation with temperature for the hydrophilic polyelectrolyte is negligible: 6.10^{-3} when passing from 298 °K to 328 °K. This agrees with our findings of the total structure function independent of temperature for hydrophilic AMAMPS in water.

IV-1-b- Effect on a hydrophobic polyelectrolyte

Concerning the hydrophobic polyelectrolyte, the slightly decrease of the scattered intensities at the intermediate charge fractions with temperature shows that the solvent quality becomes slightly better. A similar behaviour i.e. a dependence of the peak height with temperature, was also observed with a solvophobic polyelectrolyte, poly[2(methacryloyloxy)ethyltrimethylammonium 1,-1,2,3,3,-pentacyanopropenide] (abbreviated MPCP) in acetonitrile which is a poor solvent for the methacrylate backbone. [11] This evolution of the scattered intensity is less pronounced as *f* increases; the height and the position of the peak still depend on temperature as for lower *f*. For the highly charged fractions i.e. $f = 0.82$, the evolution is much weaker. It is actually different depending on the range of q:

- in the range $q \sim q^*$, the intensity of the peak remains constant with temperature for $f = 0.82$, as already observed by Boué and co [24] for the fully charged PSS ($f = 1$).
- in the asymptotic domain where $q > 0.1$ Å^{-1}, all the scattering profiles coincide for all charge fractions in the studied temperature range, indicating that the monomer-monomer correlations are independent of temperature and charge fraction *f*.
- at intermediate *q* range ($q < 0.1$ Å^{-1}), however the scattered intensity decreases slowly as a function of temperature. This includes the domain of existence of the "second shoulder"[12], observed either in log-log plot, or enhanced in the $q^2S(q)$ representation. The height of this shoulder (not shown here) depends on temperature. Note that it corresponds in form factor measurements to an oscillation which can be correlated with the size of the pearls in the pearl necklace model [13].

The scattered intensity at low q is composed of a minimum and an upturn at very low q, attributed to aggregates which are beyond the scope of this paper. When a minimum is sufficiently separated from the peak region (abscissa $q_{min} << q^*$), as in the case of $f = 0.67$ (SANS) and 0.82 (SAXS), so that it is not bound to the variation of the peak intensity, the minimum is related to the fluctuations in the semi-dilute solution, as $S(q \rightarrow 0) = kTc_p\left(\frac{\partial c_p}{\partial \Pi}\right)$.

We observe that it decreases slightly with temperature for both samples, but this can also be due to the variation of the peak intensity.

Dobrynin et al[1] have shown that sulfonated PSSNa was well described by their model in the case of a flexible polyelectrolyte in a poor solvent ($T << \Theta$). In the semi-dilute string controlled regime ($c_p < c_p^{string/bead}$), the position of the maximum in the scattering intensity q* scales as [1,4] :

$$q^* \propto \left(\frac{\left(\frac{\Theta - T}{\Theta} \right)}{\frac{l_B}{a} f_{eff}^2} \right)^{-1/4} \quad c_p^{1/2} \propto \tau^{-1/4} (\varepsilon T)^{1/4} c_p^{1/2} \qquad T< \Theta \qquad \text{(Eq.9)}$$

Θ is the theta temperature of the polymer $\left(\tau = \left(\frac{\Theta - T}{\Theta} \right) \right)$.

Concerning the peak height, it can be expressed by :

$$S(q^*) = S\left(\frac{2\pi}{\xi} \right) \approx g \approx c_p \xi^3 \qquad \text{(Eq.10)}$$

Where g is the number of monomer inside the correlation blob. [1] In the case of flexible polyelectrolyte in poor solvent [4] :

$$S(q^*) \propto \left(\frac{\Theta - T}{\Theta} \right)^{3/4} (\varepsilon T)^{-3/4} c_p^{-1/2} \qquad \text{(Eq.11)}$$

To take into account the evolution of the solvent dielectric constant ε with temperature in the range between 0 and 100 °C, [29] ε is expressed as previously in the form of a scaling law, by equation 5. However, we have seen above that this variation of ε(T) has no influence on f_{eff} in the hydrophilic case (namely $\varepsilon T \sim f_{eff}$ is a constant); which is the situation of reference [1] for the electrostatic repulsions of the chain before any formation of pearls. So it is consistent with the model to neglect it.

Neglecting such variation, the model predicts that:

- the position of the maximum in the scattering intensity q^* scales as:

For T < Θ,

$$q^* \propto \left(\frac{\Theta - T}{\Theta} \right)^{-1/4} c_p^{1/2} \qquad \text{for } c_p < c_p^{\text{string/bead}} \qquad \text{(Eq.12)}$$

For T < Θ, the evolution of the maximum in the scattering intensity q* with temperature is very weak and will depend on Θ value, which is unknown in our case. Experimentally, it was found that for the hydrophobic PSS, the peak abscissa scattering intensity q* is also independent of the temperature.

For SANS, this variation is less than 9 % for f = 0.37, in other terms a variation of 32% for (T-Θ). For f = 0.67 the peak abscissa is larger, suggesting a better solvent (decrease of Θ). It is also slightly increasing with T. The representation of q^{*-4} as a function of T gives a straight line (Figure 7a) in agreement with Eq.12 to the power of 4 ($q^{*-4} \propto \left(\frac{\Theta - T}{\Theta} \right) c_p^{-2}$) and its intersection with the x-axis gives the Θ value. For PSS f = 0.37, we find a Θ value of about

227°C (with a bad correlation coefficient) and for PSS $f = 0.67$, the Θ value is of about 141°C. These values must be taken with a lot of caution. In particular the variation of q* is of order of the experimental accuracy and precise checks of the evolution of Θ with the charge fraction would require a larger set of data and more extensive analysis.

- the maximum of the scattered intensity can be expressed as:

$$S(q^*) \propto \left(\frac{\Theta - T}{\Theta}\right)^{3/4} c_p^{-1/2} \qquad \text{(Eq.13)}$$

Since it scales like ξ^3 (Eq. 10). The weak decrease of the peak intensity I(q*), observed experimentally, as the temperature increases for PSS, is in qualitative agreement with the pearl necklace model. [1,2,4] The representation of $S(q^*)^{4/3}$ as a function of T gives a straight line (Figure 7b) in agreement with Eq.13 to the power of 4/3 ($S(q^*)^{4/3} \propto \left(\frac{\Theta - T}{\Theta}\right) c_p^{-0.66}$) and its intersection with the x-axis gives the Θ value. We find for PSS $f = 0.37$ a Θ value of 211°C and for PSS $f = 0.67$, Θ = 143°C.

-the maximum in the scattering intensity q^* multiplied by the maximum of the scattered intensity expression $S(q^*)$ can be expressed according to Eq.12 and Eq.13, ($(q^*S(q^*))^2 \varepsilon T \propto \left(\frac{\Theta - T}{\Theta}\right)$). The corresponding representation as a function of T gives a straight line (Figure 7c) and its intersection with the x-axis gives the Θ value. We find for PSS $f = 0.37$ a Θ value of 200 °C and for PSS $f = 0.67$, Θ = 136°C.

So the three methods of calculations give similar Θ values.

These variations show that the polyelectrolyte does not undergo a phase transition upon temperature in this range, but rather the solvent gets better (temperature is closer to Θ temperature).

- The scattered intensity at zero angle *S(q→0)* should scale, within the framework of Dobrynin model [1] and by taking usually in to account of the variation of ε with temperature, as :

$$S(0) \propto \frac{1}{f_{eff}} \propto \frac{l_B}{a} \propto \frac{e^2}{\varepsilon kTa} \propto \frac{1}{\varepsilon(T)T} \propto T^{0.47} \qquad \text{(Eq.14)}$$

So, the scattered intensity at zero angle *S(q→0)* should be independent of temperature, because the variation of S(0) with $T^{0.47}$ is weak in the explored range of temperature. Experimentally, we found that *S(q→0)* increases slightly with T in SAXS for the PSS but it decreases slightly in SANS, and it can be influenced of the peak scattering. So it is difficult to conclude. It is possible that the decrease of "the gap" (the difference between the maximum

and the minimum) would be a more accurate characterization. Indeed it appears well related with the solvent quality (stronger gap at high quality). At this stage calculations of the scattering using an appropriate model would be convenient and may be quite productive, but this is beyond the scope of this paper.

As a conclusion, the polyelectrolyte becomes increasingly insensitive to the effect of temperature as the charge fraction increases. For the hydrophobic polyelectrolytes, the structure of the semi-dilute polyelectrolyte solutions depends very weakly on temperature showing that the solvent quality is slightly improved with increasing T (closer to Θ), in qualitative agreement with de Gennes [7] and Dobrynin [1,2,4] models, but it seems that we are still far from Θ.

IV-2- Viscometric study in dilute and semi-dilute unentangled regimes

IV -2-a- Hydrophilic polyelectrolyte

The viscosity of polyelectrolyte solutions in semi-dilute unentangled regime can be described by the evolution of the $1/\eta_{red} = f(c_p^{1/2})$. We will use this representation giving often a linear variation in practice and has been justified formerly by the Fuoss law, which turns out to be purely empirical. The Fuoss law [30] (equation 15) is however recovered by the theory of Dobrynin and al for hydrophilic polyelectrolytes [1] and is frequently used to determine the intrinsic viscosity values [η] for polyelectrolytes in aqueous solution.

$$\frac{1}{\eta_{red}} = \frac{1}{[\eta]} + \frac{C}{[\eta]} c_p^{0.5} = \frac{1}{[\eta]}(1 + C c_p^{0.5}) \qquad \text{(Eq. 15)}$$

with η_{red} : reduced viscosity (L/mole)

[η] : intrinsic viscosity (L/mole)

C : constant ((L/mole)^{0,5})

c_p : molar concentration (moles/L)

The representation of $1/\eta_{red}$ versus $c_p^{0.5}$, for the AMAMPS f = 0.95 in water gives the same linear evolution for all the temperatures (Figure 8a). The intercept of this line gives the inverse of the intrinsic viscosity. The intrinsic viscosity extrapolated for this polyelectrolyte is equal to 370.3 L/ mole and it is independent of temperature in the range between 25 °C and 55 °C.

Moreover, we have also used for this polyelectrolyte, the representation of the specific viscosity η_{sp} versus $c_p^{0.5}$ (figure 8b) which allows a test of the theory by Dobrynin and al for hydrophilic polyelectrolytes. Indeed, the data show two linear regimes; a first regime followed by a second one with a stronger dependence with the concentration, the slope ratio between the two regimes is of the order of 3, as expected by the theory of Dobrynin and al [1]

and the intersection of the two power laws gives the concentration threshold for entanglement which is about 0.09 mole/L for this polyelectrolyte. This concentration for entanglement should be higher than 0.077 mole/L which is the value obtained by Krause and al [32] for an AMPS of higher molecular weight M_w of 950,000 g/mole, since the entanglement concentration c_e increases when M_w decreases. Our findings are thus in agreement with Krause and al [32].

IV -2-b- Hydrophobic polyelectrolyte

For the hydrophobic polyelectrolyte, the usual polyelectrolyte behavior with concentration is observed for all PSS charge fractions. Its variation with charge fraction can be explained by an increase of the hydrodynamic volume associated to the polyelectrolyte chain, as the charge fraction increases. The pearls vanish and the chain unfolds, thus expands. This agrees with the observed increase of the radius of gyration of the chain as a function of the degree of sulfonation. [13] The experimental results were fitted according to the theoretical Fuoss law [30] and the corresponding representation is on Figure 9a. The inverse of the reduced viscosity varies linearly with the square root of concentration for all the charge fractions, which is in agreement with the Fuoss law. The intercept value decreases as the charge fraction increases what gives an intrinsic viscosity that increases as the charge fraction increases. We have also used the representation of the specific viscosity η_{sp} versus $c_p^{0.5}$ (figure 9b); it gives a linear evolution for all the charges fractions with a slope that increases as the charge fraction increases, yielding to the same conclusion as previously i.e. the solvent quality is improved as the charge fraction increases (Table 1). No change of slope was observed showing that these viscosity data are below the entanglement concentration, dealing so with the semi-dilute unentangled regime, contrary to the former case.

The effect of the temperature on the viscosity behaviour shows a small increase with the temperature. The analysis of these experimental results, first for PSS (f = 0.90) through the Fuoss law[30] gives a constant value of the intrinsic viscosity with the temperature, [η] = 1666,6 L/mole. For the lower charge fractions, the viscosity increases with temperature as the charge fraction decreases. This result shows an increase of the hydrodynamic volume of the PSSNa with temperature, attributed to a slight improve of the solvent quality with temperature. This behaviour is as much marked as the charge fraction is lowered. So, the polyelectrolyte becomes increasingly insensitive to the effect of temperature as the charge fraction increases. Fuoss law[30] was applied to the experimental results that fit well with this law. The extracted intrinsic viscosity increases slightly with temperature for these hydrophobic polyelectrolytes at intermediate charge fractions. We have also used the representation of the specific viscosity

η_{sp} versus $c_p^{0.5}$ that gives a linear evolution ($\eta_{sp} = P c_p^{0.5}$) for the different temperatures with a prefactor P that increases as the temperature and the charge fraction increase. These values of P are grouped in table 1. We should note that if we take the Fuoss equation and we neglect 1 compared to $Cc_p^{1/2}$, we would find that P = [η] /C. However we keep P here as a direct experimental parameter.

Figure 10 summarizes the evolution of the intrinsic viscosity with temperature for all the charge fractions. Although the increase of the intrinsic viscosity for the PSSNa *f* = 0.35 as a function of temperature appears to be substantial, the viscosity value reached remains much lower than that of PSSNa *f* = 0.50 and *f* = 0.90. The solvent quality has been improved, but not enough to make it a good solvent, because the temperature increase does not lead to sufficient structural changes. This effect is also observed for f = 0.50

One of the aims of the paper was to compare results on the structure from Small Angle Scattering and from viscosity measurements. We find a good correlation: when the scattering reveals an evolution towards a better solvent, this evolution is nicely confirmed by the viscosity measurements. Increasing *f* (the degree of sulfonation), equivalent to making the solvent better, gives more expanded chains and larger viscosity. The same trends are found with increasing T at given *f* of both the chain degree of expansion and its viscosity, but this variation with T is much more restricted. Therefore the viscous properties of the solution can be explained by its structure as seen by scattering.

The following conclusions are listed in table 2.

V-CONCLUSION:

We have shown in this study the influence of the temperature on the structure of the aqueous hydrophobic polyelectrolyte solutions both by Small Angle Scattering and viscosity measurements. These methods appear complementary and show a fair correlation. Indeed, the peak height of the structure function for aqueous PSS solutions at intermediate charge fractions is slightly sensitive to temperature and the corresponding intrinsic viscosity increases slightly with temperature. This evolution is more pronounced as the charge fraction is lowered i.e. the hydrophobicity is increased. This behaviour indicates that partially sulfonated PSS as a hydrophobic polyelectrolyte does not undergo a phase transition upon temperature and remains in the same type of conformation, but rather the solvent quality is slightly improved with the temperature. The temperature is thus not a powerful parameter that can improve significantly the solvent quality and modify the solution structure of an hydrophobic polyelectrolyte, at least this particular one, partially sulfonated PSS. In

agreement with that, the behaviour is clearly different for hydrophilic polyelectrolytes studied here, AMAMPS and the fully charged PSSNa. Indeed, the structure function and the intrinsic viscosity of these two polyions remain strictly constant with temperature. All these experimental findings are in qualitative agreement with the theoretical pearl necklace model for hydrophobic polyelectrolytes. Water becomes a bad solvent for PSS as soon as f is reduced by a few 10%, which is likely to be due to the fact that non sulfonated poly(styrene) is very strongly hydrophobic. Things could be different with polyelectrolytes for which water would be a real theta solvent for non charged sequences. However, even in the particular situation of PSS, the strong difference between sulfonated and non sulfonated sequences is smoothed down, which could be considered as surprising : by consequence partially sulfonated polystyrene is satisfyingly described by the pearl necklace model even with respect to its temperature dependence.

As an extension of this work, it will be interesting to investigate the viscosity behaviour of this hydrophobic polyelectrolyte in a less solvophobic situation, namely in a better solvent such as DMSO which is a polar organic solvent with a high dielectric constant.

V-REFERENCES :

(1) Dobrynin, A. V.; Colby, R. H.; Rubinstein, M. *Macromolecules* **1995**, 28, 1859.

(2) Dobrynin, A. V.; Rubinstein, M.; Obukhov, S. P. *Macromolecules* **1996**, 29, 2974.

(3) Kantor,Y; Kardar, M. *Europhys.Lett*. **1994**, 27, 643.

(4) Dobrynin, A.V.; Rubinstein, M. *Macromolecules*, **1999,** 32, 915.

(5) Essafi, W.; Lafuma, F.; Williams, C.E. *J. Phys.* II **1995,** 5, 1269.

(6) Essafi, W.; Lafuma, F.; Baigl, D.; Williams, C.E. *Europhys. Lett*. **2005**, 71, 938.

(7) de Gennes P.G.; Pincus P.; Velasco R. M.; Brochard F., *J. Phys.(Paris)* **1976**, 37**,** 1461.

(8) Nierlich, M ; Williams, C.E.; Boué, F; Cotton, J.P.; Daoud, M.; Farnoux, B.; Jannink, G.; Picot, C.; Moan, M.; Wolff, C.; Rinaudo, M.; de Gennes P.G. *J. Phys. France* **1979**, 40, 701.

(9) Jannink, G. *Makromol. Chem., Macromol. Symp.* **1986**, 1, 67.

(10) Essafi, W.; Lafuma, F.; Williams, C.E. Eur. Phys. Journal B, **1999**, 9, 261.

(11) Waigh, T.A.; Ober, R.; Williams, C.E.; Galin, J.C. *Macromolecules*, **2001**, 34, 1973.

(12) Essafi, W.; Lafuma F.; Williams, C. E. *in Macro-ion Characterization. From Dilute solutions to complex fluids*, K.S. Schmitz, ed., ACS Symposium Series 548, 278, **1994**.

(13) Spiteri, M.N; Ph.D, Orsay, **1997** and Spiteri, M.N; Williams, C.E; Boué, F. *Macromolecules* **2007**, 40, 6679.

(14) Baigl, D.; Ober R.; Dan Qu, D.; Fery, A.; Williams, C. E. *Europhys. Lett*. **2003**, 62, 588.

(15) Dan Qu, D.; Baigl, D.; Williams, C.E.; Möhwald, H.; Fery, A. *Macromolecules* **2003**,36, 6878.

(16) Oosawa F., *Polyelectrolytes*; M.Dekker, New York: New York **1971**.

(17) Manning G. S. *J. Chem. Phys*. **1969**; 51, 924 and 934.

(18) Alexei Chepelianskii, Farshid Mohammad-Rafiee, Elie Raphael On the effective charge of hydrophobic polyelectrolytes arxiv.org/abs/0710.2471.

(19) Aseyev, V.O.; Tenhu, H.; Klenin, S.I. *Macromolecules* **1998**, 31, 7717.

(20) Aseyev, V.O.; Klenin, S.I.; Tenhu, H.; Grillo, I.; Geissler, E. *Macromolecules* **2001**,34, 3706.

(21) Essafi W., Spiteri M. N., Williams C., Boué F., *Macromolecules* **2009**, 42, 9568.

(22) Jousset. S, Bellissent H, Galin J.C, *Macromolecules*, **1998**, 31, 4520.

(23) Dobrynin, A.V.; Rubinstein, M. *Macromolecules* **2001**, 34,1964.

(24) Boué, F; Cotton, J.P; Lapp, A; Jannink, G. *J.Chem.Phys* **1994,** 101, 2562.

(25) Makowski, H. S; Lundberg, R. D; Singhal, G. S., U.S Patent 3 870 841, **1975** to Exxon Research and Engineering Company.

(26) Baigl, D.; Seery, T. A. P.; Williams, C. E. *Macromolecules* **2002**, 35, 2318.

(27) Mc Cormick C. L.; Chen G. S. *J. Polym. Sci. Polym. Chem. Ed.* **1982**, 20, 817.

(28) Cotton J.P. Comment faire une calibration absolue des mesures de DNPA; LLB Web site, www-llb.cea.fr

(29) Handbook of Chemistry and Physics, 76th ed.; Lide, D. R., Ed.; CRC Press: Boca Raton, FL, 1996.

(30) Fuoss R. M., Strauss UP. *Journal of Polymer Science* **1948**, 3, 246.

(31) Dragan S., Miahai M., Ghimici L. *European Polymer Journal* **2003**, 39, 1847.

(32) Krause W. E., Tan J.S., Colby R. H. *Journal of Polymer Science: Part B: Polymer Physics* **1999**, 37, 3429.

Figure and Table Captions :

Figure 1: The chemical structure of the used polyelectrolytes.

Figure 2: SAXS profiles as a function of temperature for AMAMPS $f = 0.40$, $f = 0.60$ and $f = 0.95$. The polyelectrolyte concentration $c_p = 0.32$ mole/L.

Figure 3: Normalized SAXS profiles as a function of temperature for NaPSS $f = 0.35$ and $f = 0.82$ **(a)** and absolute SANS structure function $S(q)$ as a function of q for different temperatures for PSSNa $f = 0.37$ and $f = 0.67$ **(b)**. The polyelectrolyte concentration is $c_p = 0.32$ mole/L.

Figure 4: Evolution of the reduced viscosity in water with polyelectrolyte concentration, as a function of temperature, for AMAMPS $f = 0.95$.

Figure 5: Evolution of the reduced viscosity versus the concentration, for PSSNa in water at 25°C.

Figure 6: Evolution of the reduced viscosity in water with polyelectrolyte concentration, as a function of temperature for PSSNa. **(a)** PSSNa $f = 0.90$. **(b)** PSSNa $f = 0.50$. **(c)** PSSNa $f = 0.35$.

Figure 7: Evolution of the peak abscissa q^{*-4} as a function of the temperature for PSSNa $f = 0.67$ **(a)**, that of the maximum of the scattered intensity $S(q^*)^{4/3}$ as a function of the temperature for PSSNa $f = 0.37$ **(b)** and that of $(q^*S(q^*))^2 \varepsilon T$ a function of the temperature for PSSNa $f = 0.67$ **(c)**.

Figure 8: Fit of the viscometric data on AMAMPS $f = 0.95$ in water at 25°C with the Fuoss equation **(a)** and with the representation of the specific viscosity as a function of the square root of the polyelectrolyte concentration showing the two regime viscosity concentration dependence showing two apparent regimes of viscosity concentration dependence **(b)** and allowing to determine a crossover value for entanglement concentration c_e.

Figure 9: Fit of the viscometric data on PSSNa for different charge fractions ($f = 0.35$, $f = 0.50$ and $f = 0.90$) in water at 25°C with the Fuoss equation **(a)** and with the representation of the specific viscosity as a function of the square root of the polyelectrolyte concentration **(b)**.

Figure 10: Evolution of the intrinsic viscosity as a function of temperature for PSSNa at different charge fractions, in water.

Table 1: Values of the prefactor P corresponding to the evolution of η_{sp} vs. $c_p^{0.5}$ ($\eta_{sp} = P c_p^{0.5}$) as a function of temperature for PSSNa at different charge fractions, in water.

Table 2: Summary of the results.

1-PSS

f=x/x+y

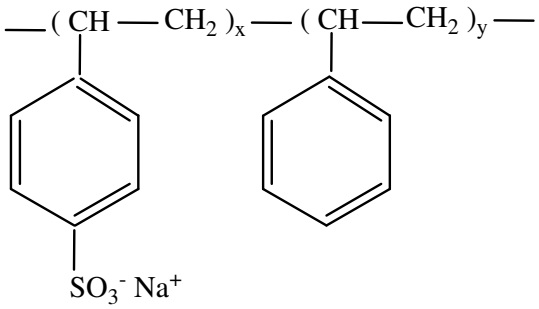

2-AMAMPS

f=x/x+y

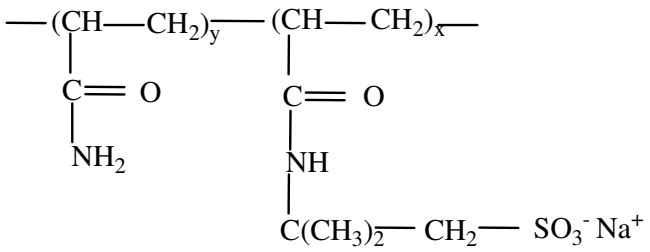

Figure 1

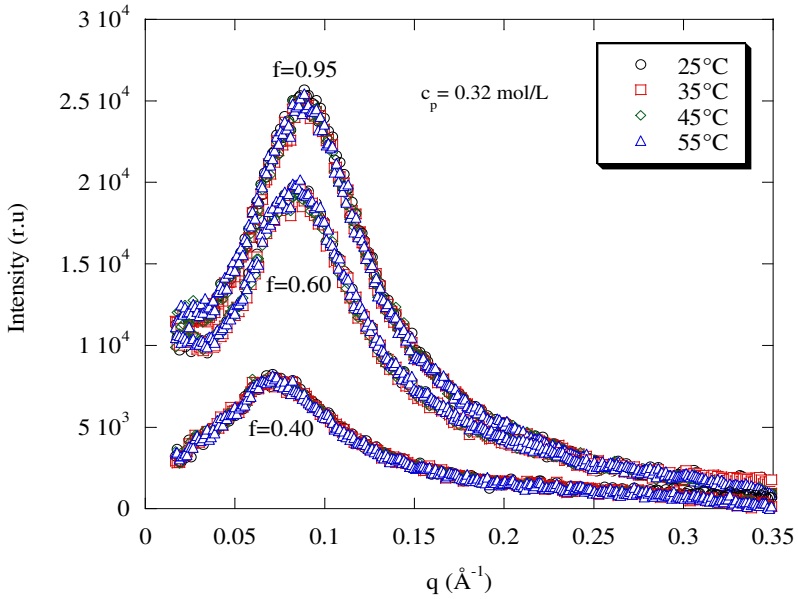

Figure 2

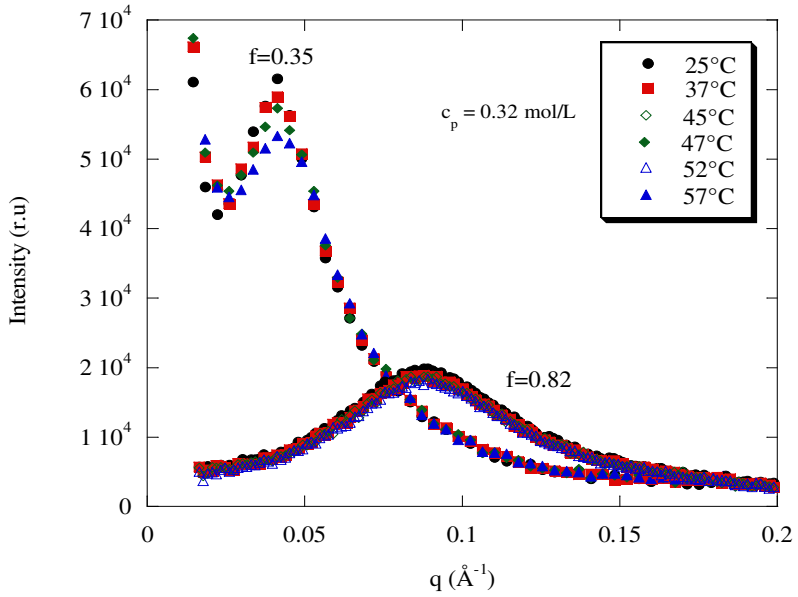
f=0.35
f=0.82
c_p = 0.32 mol/L
25°C
37°C
45°C
47°C
52°C
57°C
Intensity (r.u)
q (Å^{-1})
7 10^4
6 10^4
5 10^4
4 10^4
3 10^4
2 10^4
1 10^4
0
0
0.05
0.1
0.15
0.2

Figure 3a

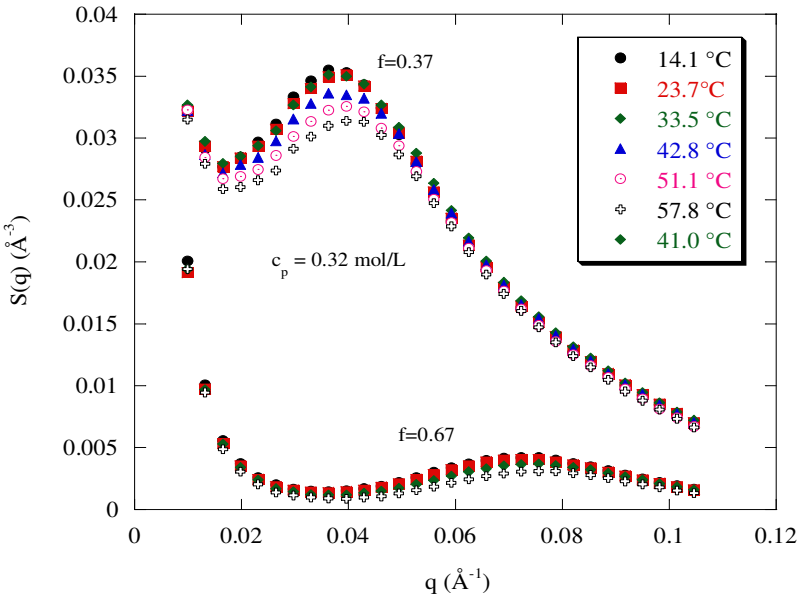
0.04
0.035
0.03
0.025
0.02
0.015
0.01
0.005
0
S(q) (Å-3)
0
0.02
0.04
0.06
0.08
0.1
0.12
q (Å-1)
f=0.37
f=0.67
cp = 0.32 mol/L
14.1 °C
23.7°C
33.5 °C
42.8 °C
51.1 °C
57.8 °C
41.0 °C

Figure 3b

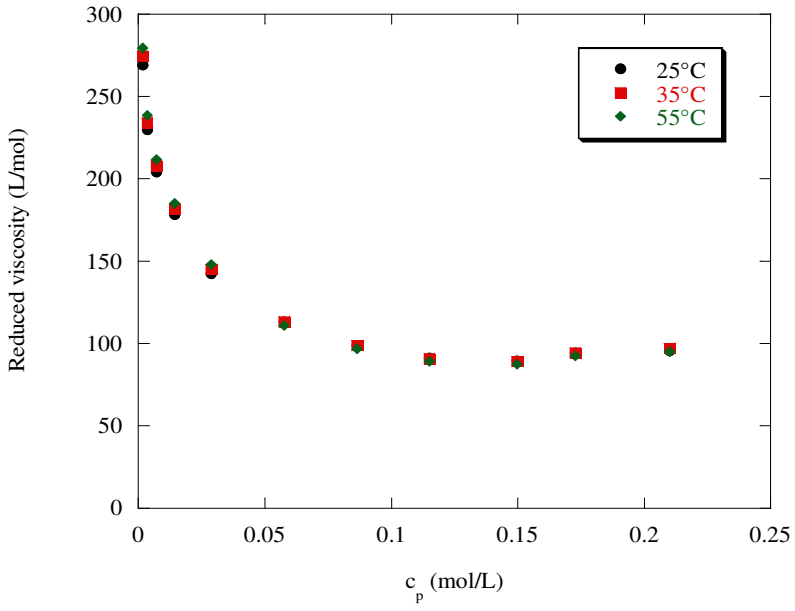
Reduced viscosity (L/mol)
300
250
200
150
100
50
0
0
0.05
0.1
0.15
0.2
0.25
c_p (mol/L)
25°C
35°C
55°C

Figure 4

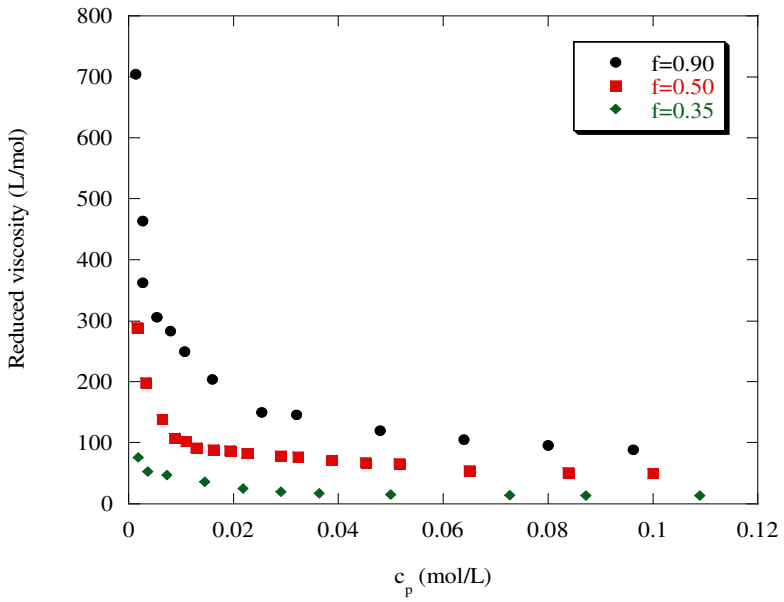
800
700
600
500
400
300
200
100
0
0
0.02
0.04
0.06
0.08
0.1
0.12
Reduced viscosity (L/mol)
c_p (mol/L)
f=0.90
f=0.50
f=0.35

Figure 5

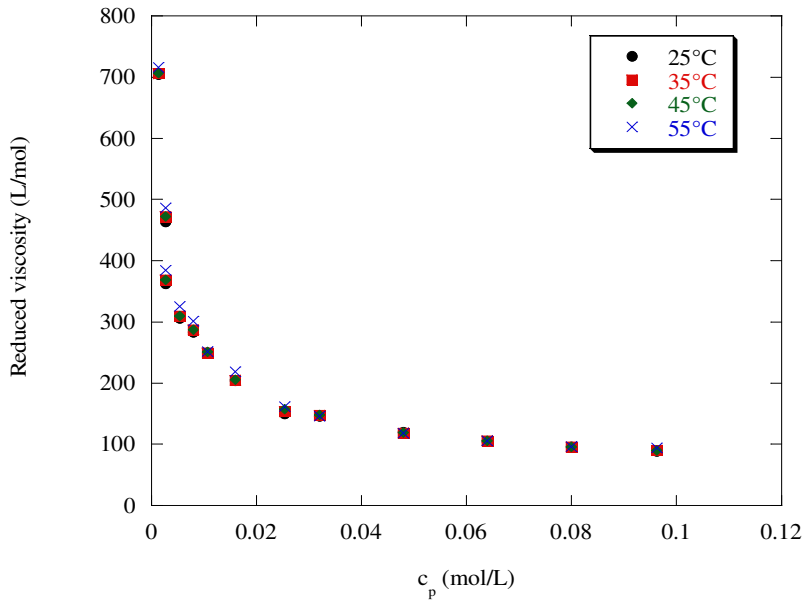

Figure 6a

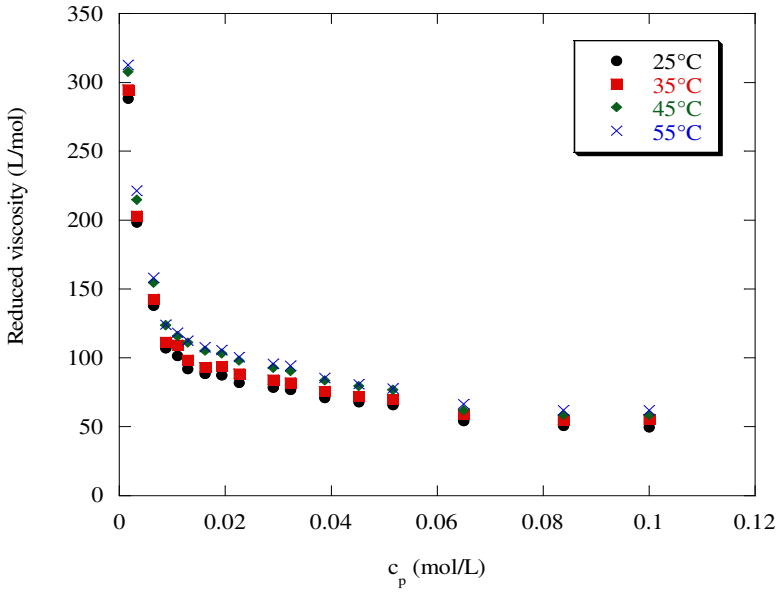

Figure 6b

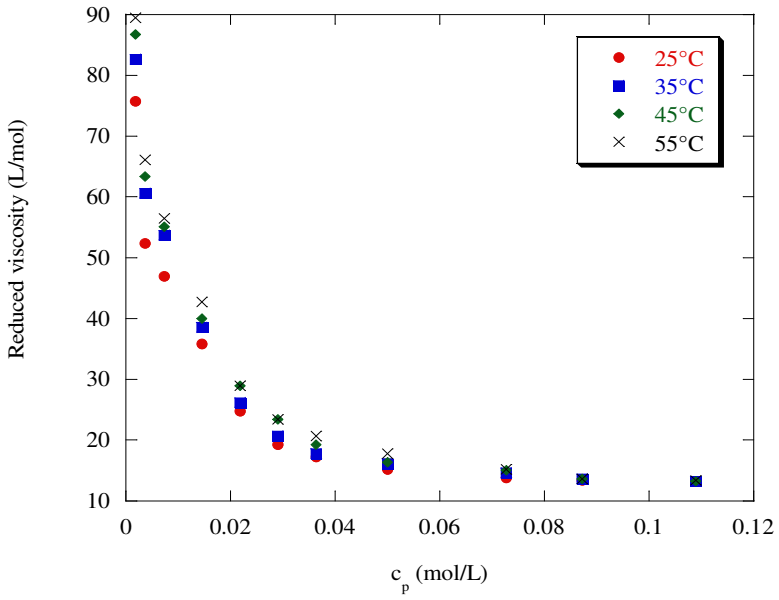
Reduced viscosity (L/mol)
90
80
70
60
50
40
30
20
10
0
0.02
0.04
0.06
0.08
0.1
0.12
c p (mol/L)
25°C
35°C
45°C
55°C

Figure 6c

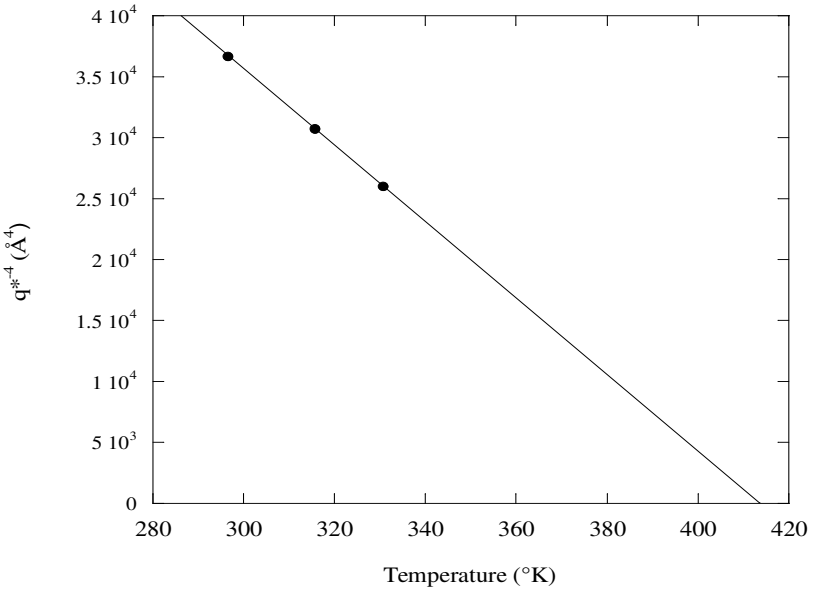

Figure 7a

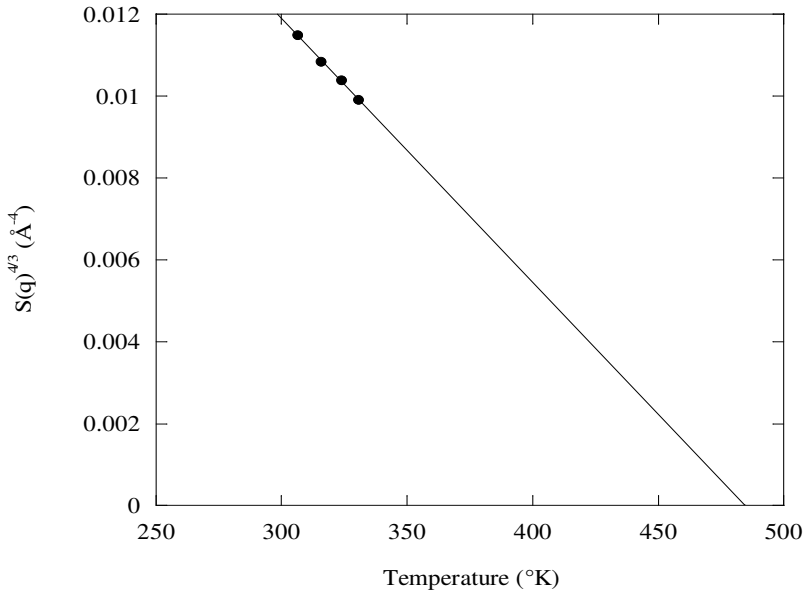

Figure 7b

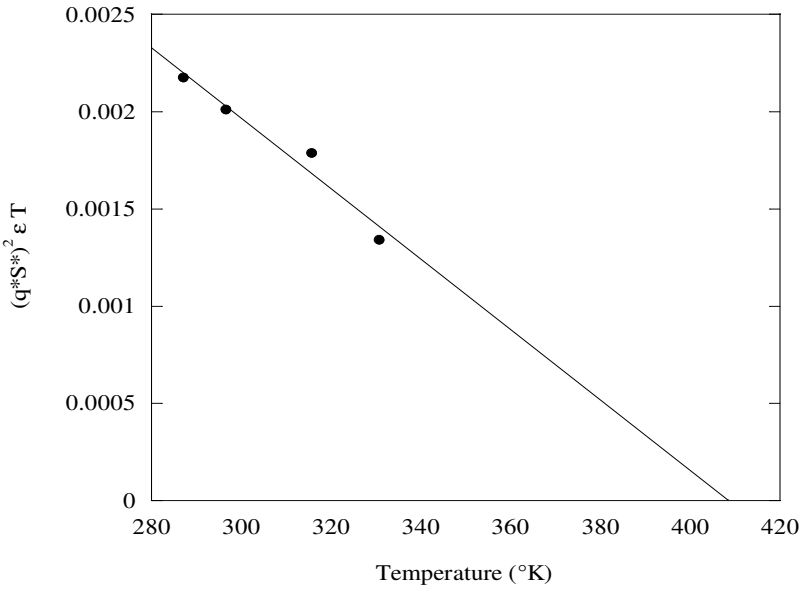
0.0025
0.002
0.0015
0.001
0.0005
0
280
300
320
340
360
380
400
420
Temperature (°K)
(q*S*)^2 ε T

Figure 7c

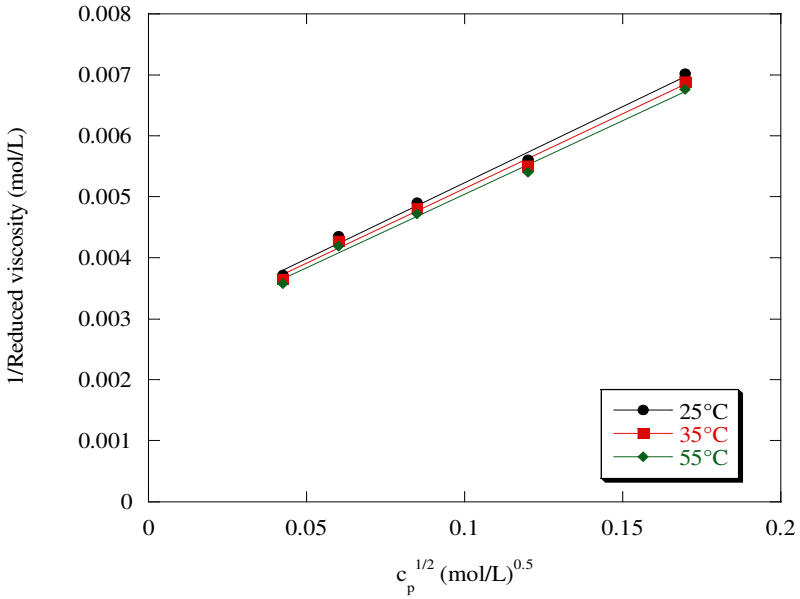

Figure 8a

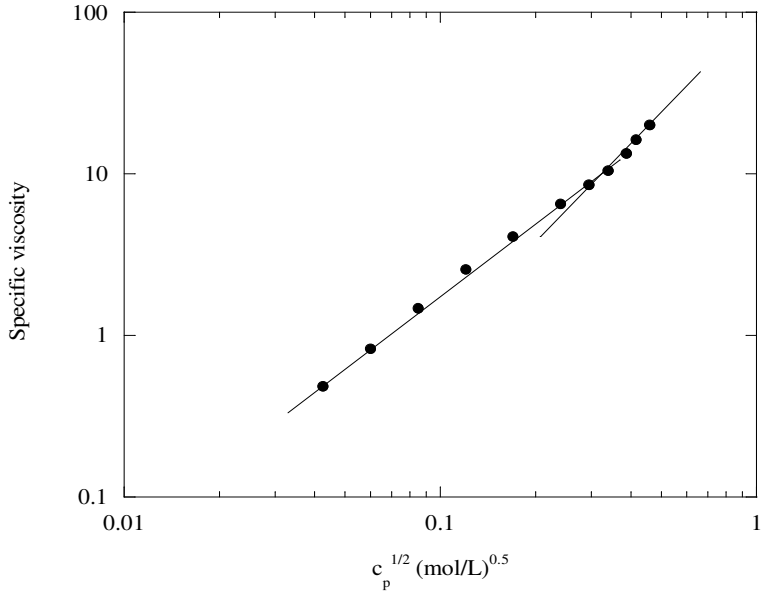

Figure 8b

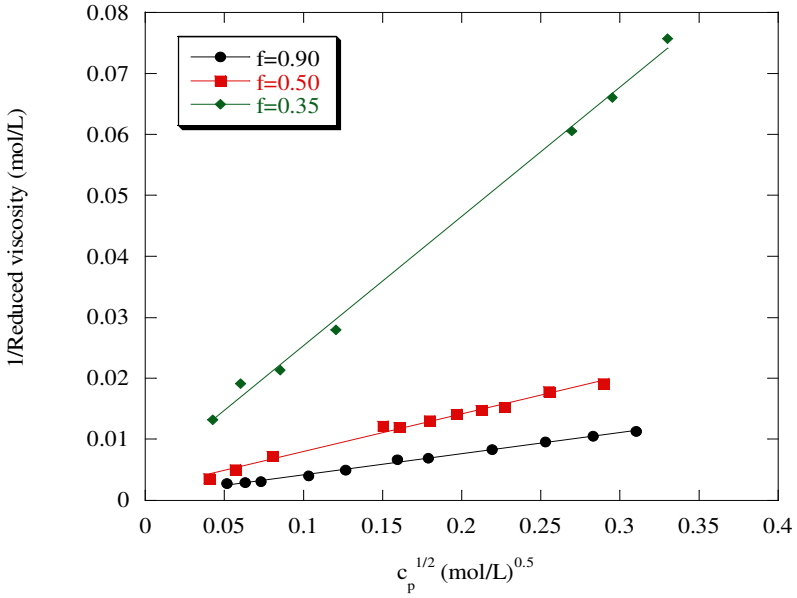

Figure 9a

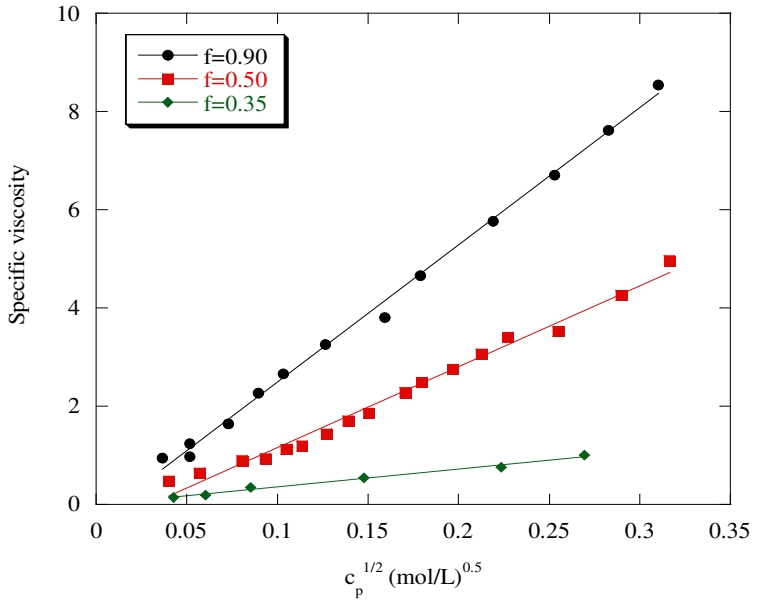

Figure 9b

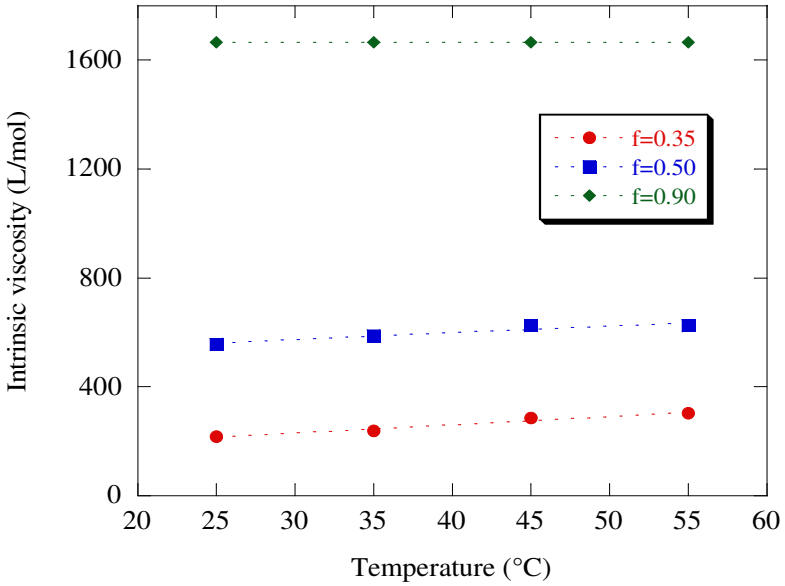
Intrinsic viscosity (L/mol)
1600
1200
800
400
0
20
25
30
35
40
45
50
55
60
Temperature (°C)
f=0.35
f=0.50
f=0.90

Figure 10

Table 1:

Temperature	P (PSSNa $f = 0.35$)	P (PSSNa $f = 0.50$)	P (PSSNa $f = 0.90$)
25	3.64	16.50	27.95
35	3.78	18.23	28.04
45	3.87	19.40	28.17
55	4.25	20.51	28.45

Table 2:

Polymer	Nature	Model tested	Scattering	Viscometry
AMAMPS	Hydrophilic	Good solvent, Only electrostatics (E)	No temperature dependence, agrees with (E)	No temperature dependence, agrees with (E)
PSS	Hydrophobic	Bad solvent, Pearl necklace model (PN)	Weak temperature dependence, agrees with (PN) still far from theta	Clear temperature dependence, agrees with (PN)